Eur. Phys. J. D **5**, 23–31 (1999)

THE EUROPEAN PHYSICAL JOURNAL D

EDP Sciences

Photoionization of the hydrogen atom in strong magnetic fields of White Dwarfs

G. Meinhardt[1], W. Schweizer[2,3,a], H. Herold[2], and G. Wunner[3]

[1] Physics Department, Faculty of Science, Naresuan University A. Muang, Phitsanulok 65000, Thailand
[2] Institute of Astronomy and Astrophysics, University of Tübingen, 72076 Tübingen, Germany
[3] Institute of Theoretical Physics I, Ruhr-University Bochum, 44780 Bochum, Germany

Received: 16 March 1998 / Revised and Accepted: 14 July 1998

Abstract. The photoionization cross-sections of the hydrogen atom in strong magnetic fields of magnetic White Dwarf stars were calculated with a direct numerical integration method using the Landau basis as a high field approach. The validity regime of these solutions overlap with those of the spherical symmetry and complement other recently developed methods. An important result is the relation between the density of states and the normalization for the more than one open channel regime leading to additional coupling terms not taken into account by multi channel quantum defect methods.

PACS. 32.60+i Zeeman and Stark effects – 97.60.-s Late stages of stellar evolution (including black holes) – 31.15.-p Calculations and mathematical techniques in atomic and molecular physics (excluding electron correlation calculations)

1 Introduction

1.1 The H-Atom in a strong magnetic field

The quantitative analysis of observed spectra of White Dwarf stars by calculating realistic synthetic spectra necessitates the knowledge of photoionization cross-sections for the hydrogen atom in strong magnetic fields. A zero order approximation was derived by Lamb and Sutherland [1], which can only be applied for modeling spectra up to 10^3 T. Potekhin *et al.* [2] discussed photoionization spectra for magnetic fields above 10^7 T and in Seipp *et al.* [3] the influence of additional electric fields are discussed.

In the presence of a strong magnetic field photoionization becomes much more complicated. For each subspace with fixed magnetic quantum number the magnetic field discretizes the continuous energy region into an infinite manifold of eigenstates. These states can be described as an overlay of Rydberg series with a magnetic splitting and shifting of the energy terms [4] or as an infinite number of Landau levels such that one Rydberg series converges to each Landau level. This latter conception is useful to describe the photoionization process at a magnetic field strength of the order of 10^4 to 10^5 T, when approached from higher field strengths. The states of each series represent the subspace of one Landau channel. Following this idea all states of the lowest Landau channel are bound states, and its Landau level corresponds to the ionization threshold. At least parts of the higher energy series are degenerate with respect to the continua of the lower Landau channels. Therefore the photoionization process can be specified as follows: after the absorption of a photon with an energy higher than the first Landau threshold, the electron occupies a state of a higher Landau level with a limited lifetime caused by its decay to the continua of lower Landau levels, hence the electron becomes a free particle.

1.2 Basic Theory

The non-relativistic Hamiltonian for the hydrogen atom in a uniform magnetic field in a symmetrical gauge reads in atomic units ($\beta = B/B_0, B_0 = 2\,\alpha\,m_e\,c^2\,/\,e\,\hbar\ \approx 4.7 \times 10^5$ T)

$$\hat{H} = \frac{\hat{p}^2}{2} + \beta(\hat{l}_z + 2\,\hat{s}_z) + \frac{1}{2}\beta^2(x^2 + y^2) - \frac{1}{r}, \qquad (1)$$

for details see [5]. (In the following we measure the energies in units of the Rydberg energy 13.6058 eV.) As the angular momentum l_z is conserved, the paramagnetic energy shift $\beta(l_z + 2s_z)$ can be separated off. Additionally it is convenient to subtract the Larmor energy $(|m| + 1)\hbar\omega_l$ with $\omega_l = e\,B\,/\,2\,m_e$. Therefore the Hamiltonian is independent of the sign of m and for each subspace with fixed magnetic quantum number m the ionization threshold is equal to $E_\infty = 0$.

As mentioned above the intensive field expansion is chosen as an ansatz for the wavefunctions, reading in terms of the Landau functions superposed by the unknown

[a] e-mail: schweizer@tat.physik.uni-tuebingen.de

channel functions in the z-direction,

$$\Psi(\varrho,\varphi,z)=\sum_{N=0}^{\infty}\Phi_{N,m}(\varrho)\,f_N(z)\,e^{\mathrm{i}m\varphi}. \tag{2}$$

The Landau functions are eigenfunctions of the cylindrical part of the Hamiltonian (1) and hence we get from equations (1, 2) the following coupled channel equations:

$$\left(-\frac{d^2}{dz^2}+4\,N\,\beta-E-V_{NN}(z)\right)f_N(z) + \sum_{N\neq N'}^{\infty}V_{NN'}(z)\,f_{N'}(z)=0, \tag{3}$$

with the coupling potentials

$$V_{NN'}(\varrho,z)=-\int_0^{\infty}\Phi_{N,m}(\varrho)\frac{2}{\sqrt{\varrho^2+z^2}}\Phi_{N',m}(\varrho)\varrho\,\mathrm{d}\varrho. \tag{4}$$

The energy thresholds for the respective channels are given by the Landau levels $E_{Landau}=4\,N\,\beta$ with $N=0,1,2\ldots$ Channels with energies smaller than the photoionization energy under consideration are called open channels.

2 The one open channel regime

2.1 Parity, boundary conditions and normalization

The starting condition is given by the conservation of the z-parity and the boundary condition of the channel solutions through the asymptotic behavior of the solution for large distances from the nucleus. For bound states the solutions converge to zero and for open channels asymptotically to a superposition of regular ($F_n(z)$) and irregular ($G_n(z)$) Coulomb functions for $l=0$:

$$\begin{aligned} f_N(z) &= a_N F_N(z)+b_N G_N(z)\\ &= a_N\sin\Theta_N+b_N\cos\Theta_N \qquad (5)\\ &= A\sin(\Theta_N+\delta_N) \qquad (6)\end{aligned}$$

$$\text{with } \sigma_0=\arg\Gamma(1+\mathrm{i}\gamma)\text{ as the Coulomb phase} \tag{7}$$

$$\text{and } \Theta=\rho-\gamma\ln 2\rho+\sigma_0, \tag{8}$$

as can be shown by an expansion of the potential leading to the field free scattering differential equation, with $\rho=\sqrt{\varepsilon}\,z$, $\gamma=-1/\sqrt{\varepsilon}$ and $\varepsilon=E-4\,N\,\beta$ [6].

The phase shift $\delta_N=\arctan(b_N/a_N)$ is a measure of the deviation between this potential and the pure Coulomb potential. In the Multi Channel Quantum Defect Theory (MQDT) this phase shift is used to interpolate transition matrix elements [7,8]. The phase shifts of the MQDT with those of the Direct Numerical Integration Method (DNIM) are in good agreement.

The normalization of the wavefunctions of the bound states can be carried out due to their quadratic integrability, $\int\psi^*\psi\,d\tau$, in contrast to the continuum wavefunctions which can only be normalized for one open channel to a box of the length L using either free wavefunctions or Coulomb functions. Then the box length, which also appears in the density of states, cancels with the L from the normalization. For more than one open channel this simple normalization looses its validity because of the relation of the normalization to the density of states.

2.2 The numerical treatment

The evaluation of the transition matrix elements can be reduced to an integration in the z-coordinate as well as for the bound-bound transitions [6,9]. To get the particular channel solutions of the coupled differential equation system (3), the coupling potential has to be calculated first using its analytical form [10,11].

The determination of the wavefunctions of the bound states as well as of the continuum states can be carried out by using ansatz (2) with N finite. The solutions can be written in a matrix scheme where the multiplication of the rows with the vector of weights give the single channels while the multiplication of the Landau functions with the single columns give the particular solutions of the coupled channel equation system.

The starting conditions for positive z-parity are:

$$\begin{aligned} f_{il}(0) &= \begin{cases}1 & \text{for}\quad i=l\\ 0 & \text{for}\quad i\neq l\end{cases} \qquad (9)\\ f'_{il}(0) &= 0,\end{aligned}$$

and for negative z-parity:

$$f_{il}(0)=0 \tag{10}$$

$$f'_{il}(0)=\begin{cases}1 & \text{for}\quad i=l\\ 0 & \text{for}\quad i\neq l\end{cases}. \tag{11}$$

If the photon energy is in the region between two higher Landau thresholds, $E_1\leq E_k<E<E_{k+1}<E_N$, the $g_1^o,\ldots,g_k^o$ are open, the $g_{k+1}^c,\ldots,g_N^c$ are closed channels. The asymptotic solutions for the open channels far from the nucleus are the Coulomb functions as mentioned above. The closed channels have to decay exponentially to zero after a certain oscillation.

In our calculations we worked with a modified Numerov method [11,13], so that the wave function at a certain point is calculated from the functions and their derivatives of the three preceding points. As the distance of neighbouring nodes of the bound state wavefunctions increases approximately quadratically, the integration steps are quadratically widened in order to minimize the necessary CPU time. The first three values were gained from the starting conditions and a Taylor expansion.

At a certain position the non-physical exponentially increasing part of the channel wave function gains more

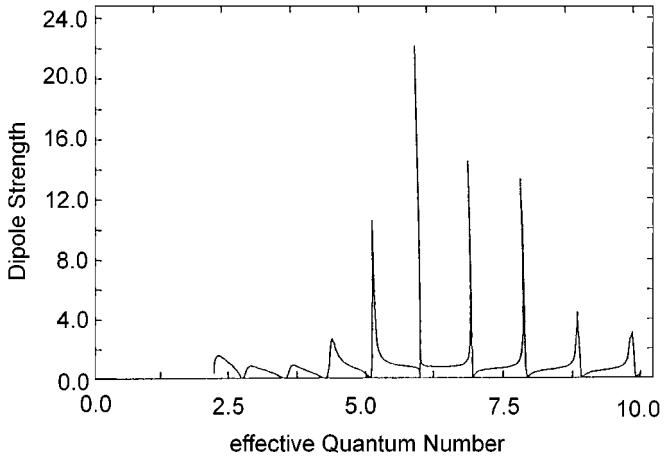

Fig. 1. Dipole strengths for the transition $\Delta m = 0$ from a state of negative z-parity, corresponding to the field free state $3d_{-1}$, to the $m^{\pi_z} = -1^+$ – subspace of continuum states in the first open channel regime $0 < E < 4\,\beta$ and $\beta = 0.05$ as a function of the effective quantum number $\nu_{\mathit{eff}} = (4\,\beta - E)^{-1/2}$, $\nu_{\mathit{eff}} = 1, \ldots, 10$.

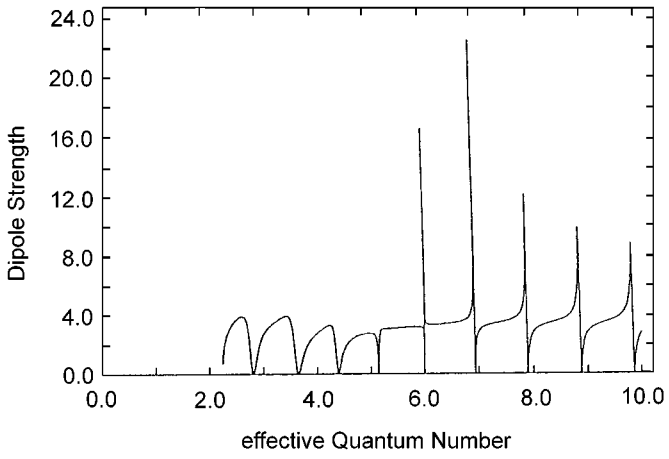

Fig. 2. Dipole strengths for the transition $\Delta m = 0$ from a state of positive z-parity, corresponding to the field free state $2p_{-1}$, to the $m^{\pi_z} = -1^-$ states as function of the effective quantum number $\nu_{\mathit{eff}} = 1, \ldots, 10$ for $\beta = 0.05$.

and more influence. Therefore, to avoid unphysical solutions, this channel has to be uncoupled at a certain position, implying that the channel is set to zero. This position can be estimated by the exponential decay of the WKB-approximation adding the z-value, z_{max}, of the greatest probability of presence, which is for channel functions identical to the maximum behind the last node. This distance is given by

$$z_{max} = \frac{1}{(4\,N\,\beta - E)}\,. \tag{12}$$

After uncoupling the channel the dimension of the matrix to be solved reduces by one. Weight factors are kept to multiply the channel solution as to making the whole solution continuous.

For $E < 0$ the channels of the bound state wave function were calculated by an energy bisection method. For $E > 0$ the open and closed channels of the wave function of the free state can be evaluated for a given value E.

Applying the Coulomb function method for normalization on a linear grid ($\Delta z = 4\beta \times 10^{-3}$) difficulties in the critical energy regions just above the ionization threshold and just below the next Landau level can be avoided by using a finer grid. Energy values of 1/1000 below the next Landau threshold could be reached.

After the calculation of the wavefunctions of both, the bound state as well as the continuum state, a numerical integration in the z-coordinate yields the transition matrix elements of all possible transitions to this m-subspace of the continuum as well as for bound-bound transitions in [9] for which the Landau expansion is valid.

2.3 Results for the first open channel regime

The results for the energy values within the interval of the ionization threshold and the first Landau level can be visualized by drawing the dipole strength (the squared transition matrix element) as a function of the effective quantum number $\nu_{\mathit{eff}} = 1/\sqrt{4\,N\,\beta - E}$, with $N = 1$ for this regime.

Using this representation the resonances should occur at the integer numbers of ν_{eff} without the coupling potentials and at small deviations from these values if the complete close coupling problem is calculated. The Rydberg structure of the resonance series can be clearly recognized for the higher values of the effective quantum number ν_{eff}. Figure 1 shows the dipole strengths of transitions from a bound state of negative z-parity corresponding to the field free $3d_1$-state to the $m = 1$-subspace of the continuum with positive z-parity. The transitions from a bound state having positive z-parity, here the field free $2p_1$ state, to the states of negative z-parity are presented in the Figures 2 and 3 and an example for the photoionization cross-section in Figure 4. Notice the shape of the resonances being peaks for an effective quantum number higher than 5 in the case of the negative to positive parity transition and higher than 6 for the other case. For low energy values the shape forms a bulge with dips at values very different from the integer values of the effective quantum numbers in contrast to the zero positions of the peak structures.

This different shape is caused by the influence of the higher channel solutions increasing with the approach to the next Landau level. The explanation of Wang *et al.* [14] that the shape is caused by the different form of the bound states for each z-parity can be only confirmed considering the spectral shape in general. The differences in detail for each subspace spectrum depend on the influence of the particular channel solutions of the continuum states.

This influence of the second channel solution becomes so predominant for transitions from the $m = 0$, negative z-parity state, that a bound state in the continuum occurs at an energy of $E = 0.157$ for a magnetic field of $\beta = 0.05$ with a lifetime comparable to that of one of the real bound states. The reason is that the high maximum of the second

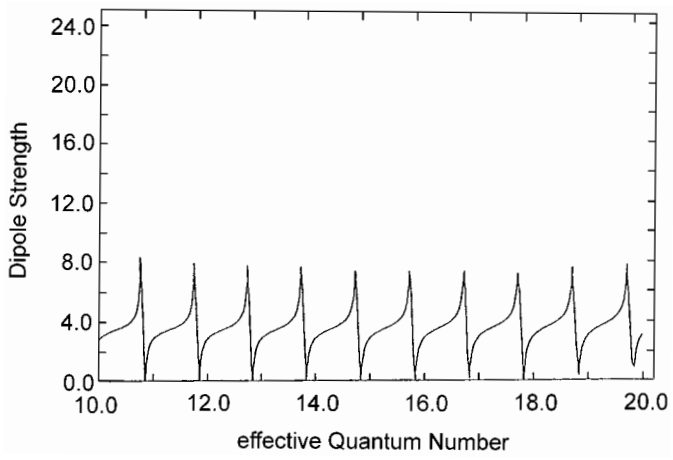

Fig. 3. Dipole strengths for the same transition as in Figure 2, but for $\nu_{eff} = 10, \ldots, 20$.

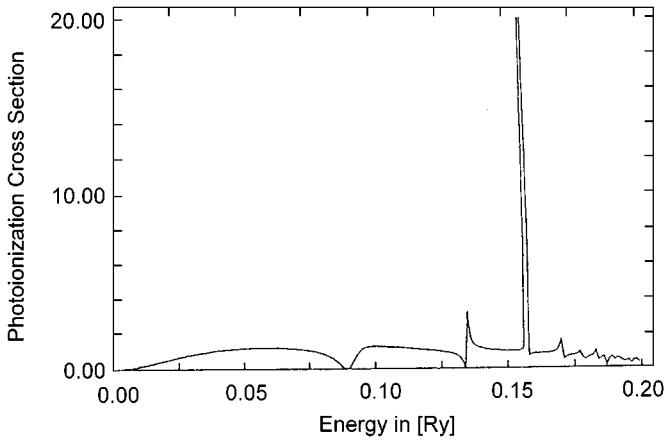

Fig. 4. Photoionization cross-sections for the transition from a state of negative z-parity, corresponding to the field free state $2p_0$ to the $m^{\pi_z} = 0^+$ continuum states for a magnetic field parameter $\beta = 0.05$ in the first open channel regime $0 < E < 4\,\beta$. The bound state occurs at an energy of $E = 0.157\mathcal{R}$.

channel solution at a distance of $35a_0$ from the nucleus increases the probability of presence in such a manner that the electron is still located close to the nucleus.

All these results gained from the DNIM represent an additional confirmation of the quantum defect theory methods [10,15]. Furthermore the DNIM provides results, such as the bound states in the continuum, which cannot be found using interpolating methods like the MQDT. But the main reason for the DNIM being more than a little improvement on other methods is the relation of the normalization of the continuum wave function to the state density for the energy regime of more than one open channel.

3 The two and more open channel regime

3.1 The relation between normalization and state density for more than one open channel solution

The continuum wave function of more than one open channel can be written as a superposition of N channels from which K are open and the remaining $N-K+1$ are closed, if the expansion is cut at N channels:

$$\Psi_f(\varrho,\varphi,z) = \sum_{i=1}^{K} \Phi_{i,m}(\varrho)\, f_i(z)\, e^{\mathrm{i}m\varphi} + \sum_{j=K+1}^{N} \Phi_{j,m}(\varrho)\, f_j(z)\, e^{\mathrm{i}m\varphi}. \quad (13)$$

For simplification the summation starts at $i = 1$ hence the threshold energy has to be changed to $E = 4(i-1)\,\beta$ and the wavelength to $k_i = \sqrt{E - 4(i-1)\beta}$. Therefore each channel wave function consists of a linear combination of N particular solutions with K open channels meeting the physical boundary conditions.

As an example, consider the simplest case in which the photon energy exceeds the second Landau level such that there are two open channels. The electron has two possibilities: either it can occupy the state where it possesses the kinetic energy

$$E_{kin} = E_{photon} - (|E_{binding}| + 4\,(i-1)\,\beta) \overset{i=1}{=} E_{photon} - |E_{binding}|$$

to circulate with the classical radius of $r = a_L\sqrt{N+1/2} = a_L/\sqrt{2}$ away from the nucleus, or it is found in the higher energy state spiraling away with a larger radius $r = a_L\sqrt{3/2}$ but less kinetic energy in the z-direction of $E_{kin} = E_{photon} - (|E_{binding}| + 4\,\beta)$.

For K open channels the oscillating part of the solutions can be combined to K linear independent wavefunctions. The total solution then reads

$$\Psi_{tot}(\varrho,\varphi,z) = \sum_{n=1}^{K} \Psi_f^{(n)}(\varrho,\varphi,z), \quad (14)$$

where $\Psi_f^{(n)} = |n\rangle$ is the same superposition of the single channels but with different weighted particular solutions to meet the correct boundary condition.

Since the density of states in the Golden Rule

$$P_{i\to f} = \frac{2\pi}{\hbar}\left|\left\langle \Psi_f \middle| \hat{W} \middle| \Psi_i \right\rangle\right|^2 \varrho(E_f) \quad (15)$$

cannot be expressed as $\varrho(E) = L/2\pi\left[(\hbar/2\,m_e)\;E\right]^{-1/2}$, a counting method had to be developed to determine the correct final density of states $\varrho_f(E) = dN_f/dE$, which is connected to the normalization of the continuum states.

For an energy interval $[E, E+\Delta E]$ the continuum wavefunctions have to satisfy the following boundary conditions if they are to be normalized to a box of length L

$$\Psi_f\left(z = \pm\frac{L}{2}\right) = 0 \Longrightarrow f_i\left(\pm\frac{L}{2}\right) = 0 \text{ for } i = 1, \ldots, K. \quad (16)$$

To fulfill these conditions an appropriate linear combination is used

$$\Psi_f = \sum_{n=1}^{K} A_n \Psi_f^{(n)} \text{ thus } f_i(z) = \sum_{n=1}^{K} A_n\, f_i^{(n)}(z)$$
$$\Longrightarrow \sum_{n=1}^{K} \left[a_i^{(n)} \cos(k_i \frac{L}{2}) + b_i^{(n)} \sin(k_i \frac{L}{2}) \right] A_n = 0. \quad (17)$$

This equation possesses a non-vanishing solution for A_n, $n = 1, \ldots, K$, if

$$\det \underline{\mathbf{M}} = 0, \text{ with } \underline{\mathbf{M}} = (M_{in})$$
$$\text{and } M_{in} = M_{in}(E) = a_i^{(n)} \cos\left(k_i \frac{L}{2}\right) + b_i^{(n)} \sin\left(k_i \frac{L}{2}\right). \quad (18)$$

$\det \underline{\mathbf{M}}(E) = 0$ determines the discrete energy values for which the channel wavefunctions with different wave vectors $\mathbf{k}$ are commensurable, that means, they have to fulfill the boundary conditions simultaneously. From the density of these energy values one can conclude the density of states as follows: for each energy value the coefficients A_n are calculated. With these coefficients the dipole strength can be expressed as

$$\left| \left\langle \Psi_f \left| \hat{W} \right| \Psi_i \right\rangle \right|^2 = \sum_{n,m=1}^{K} A_n\, A_m \left\langle \Psi_f^{(n)} \left| \hat{W} \right| \Psi_i \right\rangle \left\langle \Psi_f^{(m)} \left| \hat{W} \right| \Psi_i \right\rangle^*. \quad (19)$$

Hence the following expression has to be evaluated

$$\frac{1}{\Delta E} \sum_f A_n A_m = R_{nm},$$

with the sum over f as a sum over all states within the energy interval ΔE. Therefore equation (15) can be transformed to

$$P_{i\to f} = \frac{2\pi}{\hbar} \sum_{n,m} R_{nm} \left\langle n \left| \hat{W} \right| i \right\rangle \left\langle m \left| \hat{W} \right| i \right\rangle^*. \quad (20)$$

Hence the state Ψ_f should be normalized and the normalization included in the factors R_{nm}

$$R_{nm} = \frac{1}{\Delta E} \sum_f \frac{A_n A_m}{\| \sum_l A_l \, |l\rangle \|^2}, \quad (21)$$

where

$$\| \sum_l A_l |l\rangle \|^2 = \frac{1}{2} L \sum_{i=1}^{K} \left[\Big(\sum_l a_i^{(l)} A_l \Big)^2 + \Big(\sum_l b_i^{(l)} A_l \Big)^2 \right]. \quad (22)$$

The sums can be represented as scalar products of vectors in the n-space

$$\sum_n a_i^{(n)} A_n = \mathbf{a}_i \cdot \mathbf{A}.$$

R_{nm} then is a tensor of rank two in this space.

The vector $\mathbf{A} = (A_n)$ is uniquely fixed by the K-dimensional unit sphere, forming a unit circle for $K = 2$

$$\mathbf{A} \cdot \mathbf{A} = \mathbf{A}^2 = 1.$$

Because $\mathbf{A} \leftrightarrow -\mathbf{A}$ it is sufficient to confine the integration to the half unit sphere. The sum over the final states are transformed counting these states for a given real element $\Delta\varphi_1, \ldots, \Delta\varphi_{K-1}$ lying in this area and additional within the energy interval $E, \ldots, E + \Delta E$. $\Delta\varphi_1, \ldots, \Delta\varphi_{K-1}$ are the angles in the direction of the tangential unit vectors $\mathbf{e}_1, \ldots, \mathbf{e}_{K-1}$ which are perpendicular to the radial unit vector $\mathbf{A}/|\mathbf{A}|$.

The relation between $\mathbf{A}$ and E is provided by equation (17):

$$(\mathbf{a}_i \cdot \mathbf{A}) \cos\left(k_i \frac{L}{2}\right) + (\mathbf{b}_i \cdot \mathbf{A}) \sin\left(k_i \frac{L}{2}\right) = 0. \quad (23)$$

For the energy interval $E_0 \le E \le E_0 + \Delta E$ the wave vector k_i is expanded with respect to the energy, which results in the following expression

$$k_i \frac{L}{2} = k_{i0} \frac{L}{2} + \frac{dk_i}{dE} \xi \Big|_{E_0} = k_{i0} \frac{L}{2} + \frac{1}{2\, k_{i0}} \xi,$$

with $\xi = (E - E_0) L/2$.

Substituting this in equation (23) gives

$$\tan\left(k_{i0} \frac{L}{2} + \frac{1}{2\, k_{i0}} \xi\right) = -\frac{\mathbf{a}_i \cdot \mathbf{A}}{\mathbf{b}_i \cdot \mathbf{A}} \text{ for } i = 1, \ldots, K. \quad (24)$$

The coefficients $\mathbf{a}_i, \mathbf{b}_i$ are considered to be constant within the interval $E_0, \ldots, E_0 + \Delta E$.

Evaluating the quantities ξ_i with $i = 1, \ldots, K$ for given $\mathbf{A}$ from (24) the points $\boldsymbol{\xi} = (\xi_i)$ form an orthogonal grid with length $l_i = 2\pi k_{i0}$. Equation (24) is solved by variation:

$$\mathbf{A} = \mathbf{A} + \boldsymbol{\delta}\mathbf{A} \text{ and } \xi = \xi_i + \delta\xi_i, \quad \text{thus}$$

$$\frac{1}{\cos^2\left(k_{i0} \frac{L}{2} + \frac{1}{2\, k_{i0}} \xi\right)} \frac{1}{2\, k_{i0}} \delta\xi_i = - \frac{(\mathbf{a}_i \cdot \boldsymbol{\delta}\mathbf{A})(\mathbf{b}_i \cdot \mathbf{A}) - (\mathbf{b}_i \cdot \boldsymbol{\delta}\mathbf{A})(\mathbf{a}_i \cdot \mathbf{A})}{(\mathbf{b}_i \cdot \mathbf{A})^2}$$

$$\text{or} \quad \delta\xi_i = -2\, k_{i0} \frac{(\mathbf{b}_i \cdot \mathbf{A})\mathbf{a}_i - (\mathbf{a}_i \cdot \mathbf{A})\mathbf{b}_i}{(\mathbf{a}_i \cdot \mathbf{A})^2 + (\mathbf{b}_i \cdot \mathbf{A})^2} \boldsymbol{\delta}\mathbf{A} = - \sum_{\alpha=1}^{K-1} c_{i\alpha} \delta\varphi_\alpha \quad (25)$$

$\boldsymbol{\delta}\mathbf{A} = \sum_{\alpha=1}^{K-1} \delta\varphi_\alpha \mathbf{e}_\alpha$ represents the variation on the unit sphere. From equation (25) we get a linear equation system for $\delta\varphi_1, \ldots, \delta\varphi_{K-1}, \xi$:

$$\sum_\alpha c_{i\alpha} \delta\varphi_\alpha + \xi = \xi_i \quad \text{for} \quad i = 1, \ldots, K, \quad (26)$$

or equivalently:

$$\begin{pmatrix} \xi_1 \\ \vdots \\ \xi_{K-1} \\ \xi_K \end{pmatrix} = \underbrace{\begin{pmatrix} c_{11} & \cdots & c_{1,K-1} & 1 \\ \vdots & \ddots & \vdots & \vdots \\ c_{K-1,1} & \cdots & c_{K-1,K-1} & 1 \\ c_{K1} & \cdots & c_{K,K-1} & 1 \end{pmatrix}}_{\text{matrix} \quad \underline{\mathbf{C}}} \begin{pmatrix} \delta\varphi_1 \\ \vdots \\ \delta\varphi_{K-1} \\ \xi \end{pmatrix}.$$

Here the range of values of the angular variation is $0 \leq \delta\varphi_\alpha \leq \Delta\varphi_\alpha$ and the energy variable ξ runs from 0 to $\Delta E(L/2)$. The mapping of the angular variations to the space spanned by $(\xi_1, \ldots, \xi_K)$ *via* the matrix $\underline{\mathbf{C}}$ yields the volume $|\det \underline{\mathbf{C}}| \Delta\varphi_1 \ldots \Delta\varphi_{K-1} \Delta E(L/2)$. Dividing this volume by $(2\pi)^K k_1 k_2 \cdots k_K$ gives the corresponding number of states

$$\Delta N_f = \frac{1}{(2\pi)^K} \frac{|\det \underline{\mathbf{C}}|}{k_1 k_2 \cdots k_K} \Delta\varphi_1 \ldots \Delta\varphi_{k-1} \Delta E(L/2). \quad (27)$$

The determinant of the coefficient matrix $|\det \underline{\mathbf{C}}|$ is independent of the choice of the unit vectors $\mathbf{e}_\alpha$. As can be seen from equation (25)

$$\begin{aligned} c_{i\alpha} &= \mathbf{e}_\alpha \cdot \mathbf{c}_i, \\ \text{if } \mathbf{c}_i &= \frac{(\mathbf{b}_i \cdot \mathbf{A})\mathbf{a}_i - (\mathbf{a}_i \cdot \mathbf{A})\mathbf{b}_i}{(\mathbf{a}_i \cdot \mathbf{A})^2 + (\mathbf{b}_i \cdot \mathbf{A})^2} 2k_i. \end{aligned} \quad (28)$$

With $\tilde{\mathbf{c}}_i = \mathbf{c}_i + \mathbf{A}$, where $\mathbf{A} = \mathbf{e}_K$ as $|\mathbf{A}| = 1$ and $\mathbf{e}_K \mathbf{c}_i = 0$, it follows that:

$$\begin{aligned} \underline{\mathbf{C}} &= \left(\mathbf{e}_1, \ldots, \mathbf{e}_K\right)^T \left(\tilde{\mathbf{c}}_1, \ldots, \tilde{\mathbf{c}}_K\right), \quad \text{thus} \\ |\det \underline{\mathbf{C}}| &= \left| \det \left(\tilde{\mathbf{c}}_1, \ldots, \tilde{\mathbf{c}}_K\right) \right| \\ &= \left| \sum_{i=1}^{K} \det \left(\tilde{\mathbf{c}}_1, \ldots, \mathbf{A}, \ldots, \tilde{\mathbf{c}}_K\right) \right|. \end{aligned} \quad (29)$$

For this step $\det(\mathbf{c}_1, \ldots, \mathbf{c}_K) = 0$ could be used, because $\mathbf{c}_i \cdot \mathbf{A} = 0$ for $i = 1, \ldots, K$.

Altogether the coefficients of the mixed products of the unique states transition matrix elements are given by

$$R_{nm} = \int_{\substack{|A|=1 \\ (half)}} d^{K-1}\mathbf{A}' \times \frac{A_n A_m |\det \underline{\mathbf{C}}|}{(2\pi)^K \, k_1 \ldots \, k_K \sum_{i=1}^{K} \left[(\mathbf{a}_i \cdot \mathbf{A})^2 + (\mathbf{b}_i \cdot \mathbf{A})^2\right]} \quad (30)$$

$$\text{with } |\det \underline{\mathbf{C}}| = \left| \sum_{i=1}^{K} \det \left(\mathbf{c}_1, \ldots, \underbrace{\mathbf{A}}_{column\, i}, \ldots, \mathbf{c}_K\right) \right|$$

$$\text{and } \mathbf{c}_i = \frac{2\,k_i}{(\mathbf{a}_i A)^2 + (\mathbf{b}_i A)^2} \left[(\mathbf{b}_i A)\mathbf{a}_i - (\mathbf{a}_i A)\mathbf{b}_i\right]. \quad (31)$$

Of course it is possible to integrate over the whole unit sphere, since the integrand remains invariant for $\mathbf{A} \leftrightarrow -\mathbf{A}$.

The expression (30) for the R_{mn} was derived for K open channels. For the simplest case of $K = 2$ it will be shown how to perform the normalization using the modified density of states. The K-dimensional unit sphere becomes the two-dimensional unit circle described by the angle φ. The vector $\mathbf{A}$ can then be written as

$$\mathbf{A} = \begin{pmatrix} \cos\varphi \\ \sin\varphi \end{pmatrix}.$$

Substituting in (30) yields

$$\begin{aligned} (\mathbf{a}_i A)^2 + (\mathbf{b}_i A)^2 = N_i(\varphi) = &\left(a_i^{(1)\,2} + b_i^{(1)\,2}\right) \cos^2\varphi \\ &+ 2\left(a_i^{(1)} a_i^{(2)} + b_i^{(1)} b_i^{(2)}\right) \cos\varphi \sin\varphi \\ &+ \left(a_i^{(2)\,2} + b_i^{(2)\,2}\right) \sin^2\varphi \end{aligned} \quad (32)$$

and

$$\begin{aligned} |\det \underline{\mathbf{C}}| = \Big| &\frac{2\,k_1}{N_1(\varphi)} \left(a_1^{(1)} b_1^{(2)} - a_1^{(2)} b_1^{(1)}\right) \\ &- \frac{2\,k_2}{N_2(\varphi)} \left(a_2^{(1)} b_2^{(2)} - a_2^{(2)} b_2^{(1)}\right) \Big|. \end{aligned} \quad (33)$$

From this one gets the coefficients of the products of the transition matrix elements

$$\begin{pmatrix} R_{11} \\ R_{12} \\ R_{22} \end{pmatrix} = \frac{1}{4\pi^2 k_1 k_2} \int_0^\pi d\varphi \begin{pmatrix} \cos^2\varphi \\ \cos\varphi \, \sin\varphi \\ \sin^2\varphi \end{pmatrix} \frac{|\det \underline{\mathbf{C}}|}{N_1(\varphi) + N_2(\varphi)}. \quad (34)$$

Substituting $q = \cos\varphi$ R_{mn} can be transformed to

$$\begin{aligned} \begin{pmatrix} R_{11} \\ R_{12} \\ R_{22} \end{pmatrix} = &\frac{1}{\pi^2} \int_{-\infty}^{+\infty} dq \begin{pmatrix} q^2 \\ q \\ 1 \end{pmatrix} \\ &\times \frac{1}{\left(n_{11}^{(1)} + n_{11}^{(2)}\right) q^2 + 2\left(n_{12}^{(1)} + n_{12}^{(2)}\right) q + \left(n_{22}^{(1)} + n_{22}^{(2)}\right)} \\ &\times \left| \frac{Z_1}{n_{11}^{(1)} q^2 + 2 n_{12}^{(1)} q + n_{22}^{(1)}} - \frac{Z_2}{n_{11}^{(2)} q^2 + 2 n_{12}^{(2)} q + n_{22}^{(2)}} \right|, \end{aligned} \quad (35)$$

with

$$\begin{aligned} N_i(\varphi) &= n_{11}^{(i)} \cos^2\varphi + 2 n_{12}^{(i)} \cos\varphi \sin\varphi + n_{22}^{(i)} \sin^2\varphi, \\ Z_1 &= \frac{1}{2\,k_2} \left(a_1^{(1)} b_1^{(2)} - a_1^{(2)} b_1^{(1)}\right), \\ Z_2 &= \frac{1}{2\,k_1} \left(a_2^{(1)} b_2^{(2)} - a_2^{(2)} b_2^{(1)}\right). \end{aligned}$$

If carrying out a case distinction for $\det \underline{\mathbf{C}} > 0$ or $\det \underline{\mathbf{C}} < 0$ these terms can be integrated explicitly after a partial fraction expansion.

One additional limiting case remains to be considered. If there is no coupling between the channels, which means that $a_1^{(2)}, b_1^{(2)}, a_2^{(1)}, b_2^{(1)} \to 0$, then the integrand in (34) has to be evaluated only for $\varphi = 0$ for channel 1 and for $\varphi = \pi/2$ for channel 2. For the first channel with $\varphi \approx 0$ the determinant $|\det \underline{\mathbf{C}}|$ becomes

$$|\det \underline{\mathbf{C}}| \approx \frac{2\,k_2 \left| a_2^{(1)} b_2^{(2)} - a_2^{(2)} b_2^{(1)} \right|}{\left(a_2^{(1)2} + b_2^{(1)2}\right) + 2\left(a_2^{(1)} a_2^{(2)} + b_2^{(1)} b_2^{(2)}\right)\varphi + \left(a_2^{(2)2} + b_2^{(2)2}\right)\varphi^2}$$

and

$$N_1(\varphi) + N_2(\varphi) \approx a_1^{(1)\,2} + b_1^{(1)\,2}.$$

Setting

$$\begin{cases} a_2^{(1)} = \epsilon \cos\alpha \\ b_2^{(1)} = \epsilon \sin\alpha \end{cases} \quad \text{and} \quad \begin{cases} a_2^{(2)} = a \cos\alpha \\ b_2^{(2)} = a \sin\alpha \end{cases},$$

and $\varphi = (\epsilon/a)t$ with $\epsilon \to 0$, the conclusion is that

$$R_{11} \approx \frac{1}{2\,\pi\,k_1 \left(a_1^{(1)\,2} + b_1^{(1)\,2}\right)} \times \underbrace{\frac{1}{\pi} \int_{-\infty}^{+\infty} dt \frac{|\sin(\beta - \alpha)|}{1 + 2\cos(\beta - \alpha)t + t^2}}_{=1}. \qquad (36)$$

R_{12} and R_{22} approach zero.

In the same way the contribution of $\varphi \approx \pi/2$ becomes

$$R_{22} \approx \frac{1}{2\,\pi\,k_2 \left(a_2^{(2)\,2} + b_2^{(2)\,2}\right)}. \qquad (37)$$

The expression (36) is simply the normalization as in the case of one channel, restricted by the boundary value considerations for high z-values, as described in the former section.

3.2 Results for the more than one open channel regime

Since getting results for the more than two open channel regime will not provide any more insight but complicate the relation of normalization and state density and additionally increase the CPU-time proportional to K^2, K being the number of open channels, only the regime of two open channels $4\,\beta < E < 8\,\beta$ was considered.

The code for these calculations had to be modified so that two state functions were obtained instead of only one solution for the one open channel as outlined in the previous section. These two states can be found as a linear combination of the four open channel solutions together with the closed channels. The coefficients of the open channel solutions can be arbitrarily chosen if the linear independence of the wavefunctions of the two states is assured. These coefficients can be chosen for the first state in such a manner that the second open particular solution disappears ($A_1 = 1, A_2 = 0$), and *vice versa*, for the second state the first particular solution is eliminated ($A_1 = 0, A_2 = 1$). Hence the coefficients of the contributing solutions become equal to those of the respective Coulomb functions. The open solutions approach the respective Coulomb functions for large z-values.

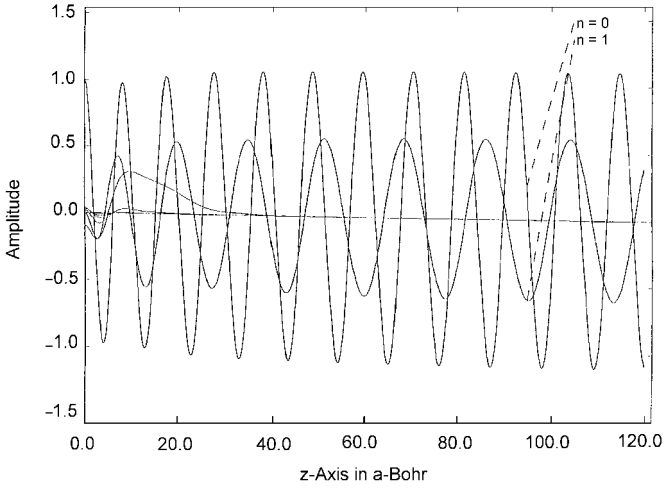

Fig. 5. The first six channel functions of the first continuum state with a positive z-parity, $m = -1$, in the two open channel regime at an energy $E = 0.3\mathcal{R}$ and a magnetic field parameter $\beta = 0.05$.

Using this linear combination of the channel functions not only the calculation of $a_{ij}^{(n)}$ can be simplified. The physical meaning of the wavefunctions of the two states only becomes evident for this representation in the Hilbert space. Figure 5 shows the first six channel solutions for the state of high kinetic energy recognizable from the small wavelength of the open nondecaying channel function with the high probability amplitude. There is also a possibility for the electron to reach the other state since the other open superposed solution represents the probability amplitude for the state with lower kinetic energy of the electron at the next Landau level. For the other state, whose first six channel solutions are shown in Figure 6 the amplitudes of the open channel solutions are rather opposite to those of the first state.

The small difference between the amplitudes cannot be the reason for the different values of the transition probability to the single electron states. The influence of the third closed channel solution, with its huge maximum for the third channel of the second state functions, is the reason that the second state is more likely occupied than the first state as can be seen in Figures 7 and 8.

The final transition probability is a superposition of both dipole strengths according to the relation (20) connecting the normalization to the state density. For the two

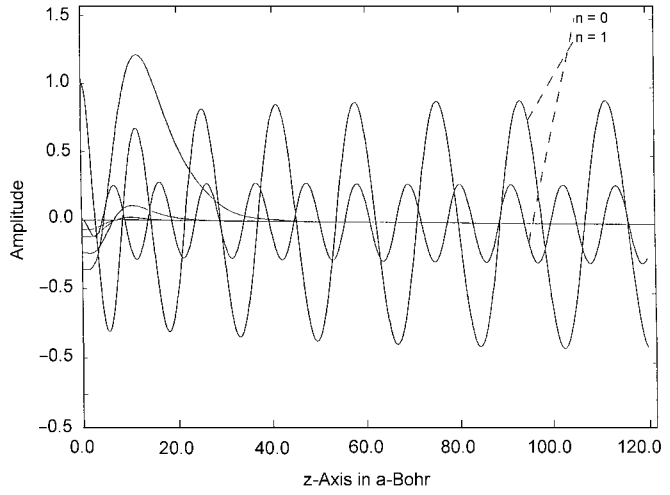

Fig. 6. The first six channel functions of the second continuum state with a positive z-parity, $m = -1$, in the two open channel regime at an energy $E = 0.3\mathcal{R}$ and a magnetic field parameter $\beta = 0.05$.

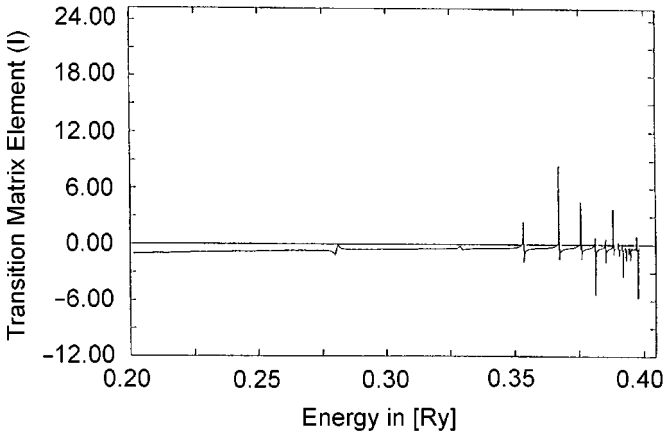

Fig. 7. Transition matrix element (I) for the transition from $m^{\pi_z} = -1^-$ ($3d_{-1}$ field free) to the first continuum state with two open channels of the subspace $m^{\pi_z} = -1^+$.

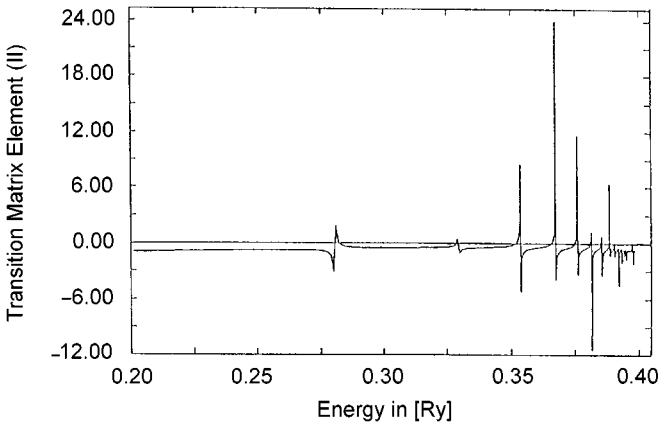

Fig. 8. Transition matrix element (II) for the transition from $m^{\pi_z} = -1^-$ ($3d_{-1}$ field free) to the second continuum state with two open channels of the subspace $m^{\pi_z} = -1^+$.

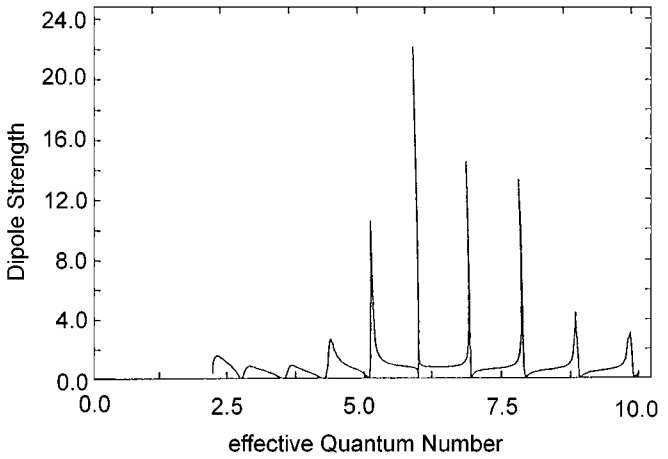

Fig. 9. Photoionization cross-sections for the transition $m^{\pi_z} = -1^-$ ($3d_{-1}$ field free) $\rightarrow$ $m^{\pi_z} = -1^+$ for the energy regime of two open channels $0.2\mathcal{R} < E < 0.4\mathcal{R}$ and a magnetic field parameter $\beta = 0.05$.

open channel regime this gives

$$P_{i\to f} = \frac{2\pi}{\hbar}\Big[R_{11}\left|\left\langle 1\left|\hat{W}\right|i\right\rangle\right|^2 + 2\mathrm{Re}\Big[R_{12}\left\langle 1\left|\hat{W}\right|i\right\rangle\left\langle 2\left|\hat{W}\right|i\right\rangle^*\Big] + R_{22}\left|\left\langle 2\left|\hat{W}\right|i\right\rangle\right|^2\Big]. \quad (38)$$

Multiplying this transition probability with the factor $4\,\pi\,\alpha\,(E_f - E_i)$, with α being the fine structure constant, gives the photoionization cross-sections. These are presented in Figure 9 as a function of energy for a magnetic field of $\beta = 0.05$, and a transition from a state with negative z-parity, the corresponding $3d_{-1}$-state without a magnetic field, to the subspace of positive z-parity.

The shape of the resonances is not so different for the higher and lower energy regions as it is for the one open channel regime. The bulges of the lower resonances become slightly peaked while the peaks of the higher energy resonances become a little smoother. The peaks of the energy region starting at about 10% of 8β below the third Landau level are not changed so much because of the decreasing influence of the third Landau channel. The channel's maximum shifts so far away from the nucleus with rising energy that there is no more overlap with the bound state solution, and so higher channels become important as in the case of the first open channel regime. Note, that the cross-section for the lower energy region does not decay to zero due to the superposition of the transition probability of two electron states.

4 Conclusions

All results presented are in excellent agreement with the photoionization cross-sections of the recent applications of the Complex Coordinate Rotation Method (CCRM) [16,17], and the MQDT [14].

The results presented by [18–20] couldn't be confirmed neither with the DNIM nor with any of the other methods. The reason for this disagreement can be found in non-decaying closed channel solutions, which cause inaccuracy in the calculation of the transition matrix element. Additionally the extension to other energy regions of an approximation which is valid only just below the first Landau threshold [21], is more than questionable.

The remaining problem is the agreement of the MQDT results to the DNIM using the new method connecting the normalization to the state density for more than one open channel. As they did not specify the normalization Wang and Greene supposedly applied the usual normalization methods to a box with the dimension L or the flux normalization throughout for all energy regimes. For the regime of two open channels the usual normalization leads to the expressions for disappearing coupling, neglecting the coupling term $R_{12} \left\langle 1 \left| \hat{W} \right| i \right\rangle \left\langle 2 \left| \hat{W} \right| i \right\rangle$ in equation (38).

The contribution of this coupling term does not exceed more than 1% of the other two terms which are taken into account by the former normalization methods, so that the error should be very small in most cases.

The CCRM of course is not affected by the normalization problem of continuum states, because the eigenvalue problem is rotated in the complex plane so that the resonances are additional solutions in this representation. In the energy regime close to the Landau levels oscillations occur using this method due to the unresolvable density of eigenvalues. In this region the DNIM could be a good complement to the complex coordinate rotation method.

We would like to thank Professor H. Ruder for his encouragement. This work was supported by the Deutsche Forschungsgemeinschaft (DFG).

References

1. F.K. Lamb, P.G. Sutherland, in *Physics of Dense Matter*, edited by C.J. Hansen, D. Deidel, Vol. 265 (Dordrecht, Holland, 1974).
2. A.Y. Pothekin, G.G. Pavlov, J. Ventura, Astron. Astrophys. **317**, 618 (1997).
3. I. Seipp, W. Schweizer, Astron. Astrophys. **318**, 990 (1997).
4. W. Rösner, G. Wunner, H. Herold, H. Ruder, J. Phys. B: At. Mol. Phys. **17**, 29 (1984).
5. H. Ruder, G. Wunner, H. Herold, F. Geyer, *Atoms in Strong Magnetic Fields* (Springer-Verlag, Heidelberg, 1994).
6. M. Abramowitz, I. Stegun, *Handbook of Mathematical Functions* (Dover Publications, New York, 1972).
7. U. Fano, A.R.P. Rau, *Atomic Collisions and Spectra* (Academic Press, New York, 1986).
8. M.J. Seaton, J. Phys. B: At. Mol. Phys. **18**, 2111 (1985).
9. H. Forster, W. Strupat, W. Rösner, G. Wunner, H. Ruder, H. Herold, J. Phys. B: At. Mol. Phys. **17**, 1301 (1984).
10. H. Friedrich, M. Chu, Phys. Rev. A **28**, 1423 (1983).
11. D. Wintgen, Ph.D. thesis, University Munich (1985).
12. C. Bardin, Y. Dandeu, L. Gauthier, J. Guillermin, T. Lena, J.M. Pernet, H.H. Wolter, T. Tamura, Comp. Phys. Comm. **3**, 73 (1972).
13. C. Froese C, Can. J. Phys. **41**, 1895 (1983).
14. Q. Wang, C.H. Greene, Phys. Rev. A **44**, 7448 (1991).
15. D. Wintgen, H. Friedrich, Phys. Rev. A **35**, 1628 (1987).
16. D. Delande, A. Bommier, J.C. Gay, Phys. Rev. Lett. **66**, 141 (1991).
17. C.-H. Iu, G.R. Welch, M.M. Kash, D. Kleppner, D. Delande, J.C. Gay, Phys. Rev. Lett. **66**, 145 (1991).
18. A. Alijah, J.T. Broad, J. Hinze, in *Atomic Spectra and Collisions in External Fields*, edited by K.T. Taylor, C.W. Clark, M.H. Nayfeh (Plenum Press, New York, 1988).
19. A. Alijah, Ph.D thesis, Universität Bielefeld (1988).
20. A. Alijah, J.T. Broad, J. Hinze, J. Phys. B: At. Mol. Opt. Phys. **23**, 45 (1990).
21. J. Dubeau, M.J. Seaton J. Phys. B: At. Mol. Phys. **17**, 381 (1984).